153.9 ± 61.8 GBq/μmol at the time of injection for [^{11}C]DASB and [^{11}C]WAY100635, respectively.

Preprocessing

A PET summation image of all frames and dynamic images were coregistered to each individual MR image by using PMOD (PMOD Technologies, Zurich, Switzerland). The individual MR image was spatially normalized to the Montreal Neurological Institute (MNI) stereotaxic brain, and subsequently, the transformation parameters were applied to the coregistered PET dynamic images. Thus, the PET and MR images of all subjects were anatomically standardized to the MNI template. Volumes of interest (VOIs) were manually delineated by a rater (H.T.) in the cerebellar cortex, dorsal raphe nuclei, thalamus, and striatum for [^{11}C]DASB, and in the cerebellar cortex and hippocampal area for [^{11}C]WAY100635, on the averaged and standardized PET summation and MR images by using the PMOD fusion tool. Circular VOIs with a diameter of 8 mm in the transaxial planes were set for the dorsal raphe nucleus from $z = -38$ to $z = -30$ in the coordinate of the MNI template. To obtain regional time-activity curves, regional radioactivity was calculated for each time frame, corrected for decay and plotted versus time.

Calculation of binding potentials and generation of parametric images for both tracers

For the PET study with [^{11}C]WAY100635, the binding potential (BP) for nondisplaceable radioligand in tissue (BP_{ND}) (Innis et al., 2007) was calculated using a reference tissue model on a voxel-by-voxel basis (Lammertsma and Hume, 1996).

$$C_T(t) = R_1 C_R(t) + \left(k_2 - \frac{R_1 k_2}{1+BP_{ND}}\right) C_R(t) \otimes \exp\left(\frac{-k_2 t}{1+BP_{ND}}\right),$$

where $C_T(t)$ is the radioactivity concentration in a brain region, and $C_R(t)$ is the radioactivity concentration in the reference region. R_1 is the ratio of K_1/K_1' (K_1, influx rate constant for the brain region, K_1', influx rate constant for the reference region), k_2 is the efflux rate constant for the brain region, and $\otimes$ denotes the convolution integral. In this analysis, three parameters (BP_{ND}, R_1, and k_2) were estimated by the basis function method (Gunn et al., 1997, 1998). The cerebellum was used as reference region because a postmortem study indicated that the cerebellum cortex is almost devoid of 5-HT_{1A} receptors (Varnas et al., 2004).

For the PET study with [^{11}C]DASB, BP_{ND} was calculated by using a multi-linear reference tissue model 2 (MRTM2) (Ichise et al., 2003),

$$C_T(T) = -\frac{V}{V'b}\left(\int_0^T C_R(t)dt + \frac{1}{k_2'} C_R(t)\right) + \frac{1}{b}\int_0^T C_T(t)dt$$

where $C_T(T)$ is the radioactivity concentration in a brain region, and $C_R(t)$ is the radioactivity concentration in the reference region. V and V' are the corresponding total distribution volumes (i.e., $V = K_1/k_2$, $V' = K_1'/k_2'$; k_2', the efflux rate constant from the reference tissue to plasma). b is the intercept term, which becomes constant for $T > t^*$. The k_2' value was estimated by the MRTM method (Ichise et al., 2002) and, to minimize the variability of k_2' estimation, a weighted mean k_2' value according to the VOI size over the raphe nucleus, thalamus, and striatum was calculated with the cerebellum as reference region, because postmortem studies indicated that the cerebellum cortex is almost devoid of 5-HTT (Kish et al., 2005; Varnas et al., 2004). BP_{ND} is then calculated from the two regression coefficients as,

$$BP_{ND} = -(\gamma_1/\gamma_2 + 1),$$

where $\gamma_1 = -V/(V'b)$ and $\gamma_2 = 1/b$, respectively.

Image data analysis

VOIs were placed on the standardized BP_{ND} images for the bilateral putamen; caudate nucleus; globus pallidus; thalamus and its subregions (pulvinar, mediodorsal, and anteriodorsal); hippocampal regions including the parahippocampus, uncus, and hippocampus; anterior and posterior cingulate; and the lateral temporal cortex, basal side as well as the convex side of the frontal cortex, parietal cortex, and occipital cortex (Fig. 1, Table I). The same VOI set was applied for both [^{11}C]WAY100635 and [^{11}C]DASB in all subjects.

Statistical analysis

Data are presented as mean ± SD. Pearson's correlation coefficient was calculated for the evaluation of correlation. Correction for multiple comparisons was not performed during the analysis because of the large number of correlations performed, and these results were considered exploratory. Laterality of the hemispheres was tested by performing a paired t-test for each region. SPSS package version 16 (SPSS, Chicago, IL) was used for statistical analysis.

RESULTS

For both radiotracers, parametric BP_{ND} images with anatomic standardization were obtained from 17 participants. The averaged images for all subjects are presented in Figures 2 and 3; mean and SD values of BP_{ND} are shown in Table II and Figure 4.

Distribution patterns of the 5-HTT and 5-HT_{1A} receptors in the human brain were measured with radioligands [^{11}C]DASB and [^{11}C]WAY100635, respectively, and they were observed to be quite different. The highest binding to 5-HTT was observed in the dorsal raphe nuclei, thalamus, and striatum. Moderate binding was observed in the insula, hippocampal area, and the anterior and posterior cingulate; very

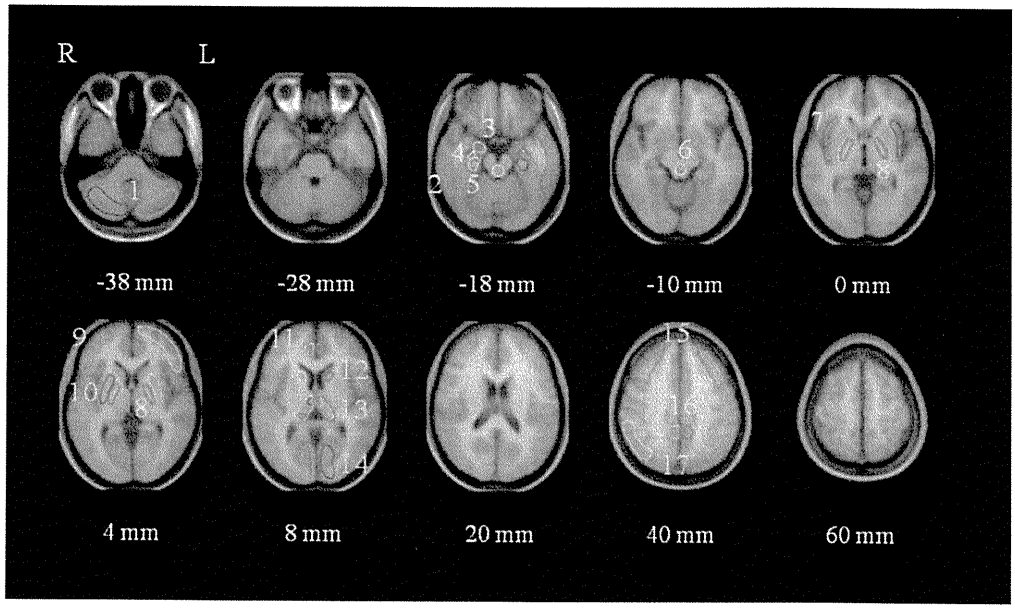

Fig. 1. VOIs drawn on the anatomically standardized MR images averaged for all subjects. Z = −38, −28, −18, −10, 0, 4, 8, 20, 40, 60 mm parallel to the anterior commissure and posterior commissure (AC-PC) line in the MNI template brain. L denotes left side of the brain; R denotes right side; 1, cerebellar cortex; 2, lateral temporal cortex; 3, uncus (amygdala); 4, hippocampus; 5, parahippocampal gyrus; 6, dorsal raphe nucleus; 7, insula; 8, globus pallidus; 9, base of frontal cortex; 10, putamen; 11, anterior cingulate; 12, head of caudate nucleus; 13, thalamus; 14, occipital cortex; 15, frontal convexity; 16, posterior cingulate; 17, parietal cortex.

TABLE I. Representative MNI coordinates and volumes in VOIs drawn on the MNI template image

	Right				Left				
Region	X	Y	Z	Volume (cm^3)	X	Y	Z	Volume (cm^3)	Total volume (cm^3)
Cerebellum	25	−70	−38	4.20	−31	−69	−38	4.30	8.50
Dorsal raphe nucleus	0	−31	−14						1.13
Striatum				1.69				1.99	3.68
Putamen	26	−1	4	1.34	−28	−2	4	1.54	2.88
Caudate head	14	14	8	0.35	−15	12	8	0.45	0.80
Globus Pallidus	20	−8	0	0.89	−18	−6	0	0.95	1.84
Thalamus	10	−23	8	1.67	−12	−22	8	1.60	3.27
Hippocampal complex				1.62				1.73	3.34
Uncus	21	−7	−18	0.70	−27	−24	−18	0.80	1.50
Hippocampus	29	−16	−18	0.19	−28	−13	−18	0.22	0.41
Parahippocampus	26	−24	−18	0.70	−27	−24	−18	0.80	1.50
Insula	38	4	−2	1.74	−38	3	−2	1.46	3.20
Anterior cingulate	5	43	8	0.53	−7	43	8	0.58	1.10
Posterior cingulate	6	−47	40	0.91	−9	−47	40	0.72	1.63
Base side of frontal cortex	34	45	4	4.58	−36	45	4	4.66	9.24
Frontal convexity	31	29	40	3.23	−35	24	40	3.25	6.51
Lateral temporal	53	−17	−18	5.58	−55	−17	−18	5.26	10.84
Occipital cuneus	13	−81	8	2.47	−9	−81	8	2.54	5.02
Parietal	49	−56	40	3.17	−51	−57	40	3.30	6.46

low binding was observed in the neocortical regions. In contrast, the highest binding to 5-HT_{1A} receptors was observed in the medial temporal regions including the hippocampus, uncus (amygdala), parahippocampus, and insula. Then, slightly lower binding was observed in the cingulate cortex and other cortical regions in descending order, with very low binding being seen in the basal ganglia and thalamus. As shown in Figure 4, when we divide brain regions into 5-HTT transporter rich regions and 5-HT_{1A} receptor rich regions, the relationships between mean values of BP_{ND} in 5-HTT and 5-HT_{1A} receptors were quite different. No linear correlation was found in 5-HTT transporter-rich regions between the mean values of BP_{ND} in 5-HTT and 5-HT_{1A} receptors, while a positive linear correlation, except the occipital cortex (r = 0.862, P = 0.006), was found between them in the 5-HT_{1A} receptor-rich regions.

There was no significant difference between the two sides of the brain with either of the radiotracers,

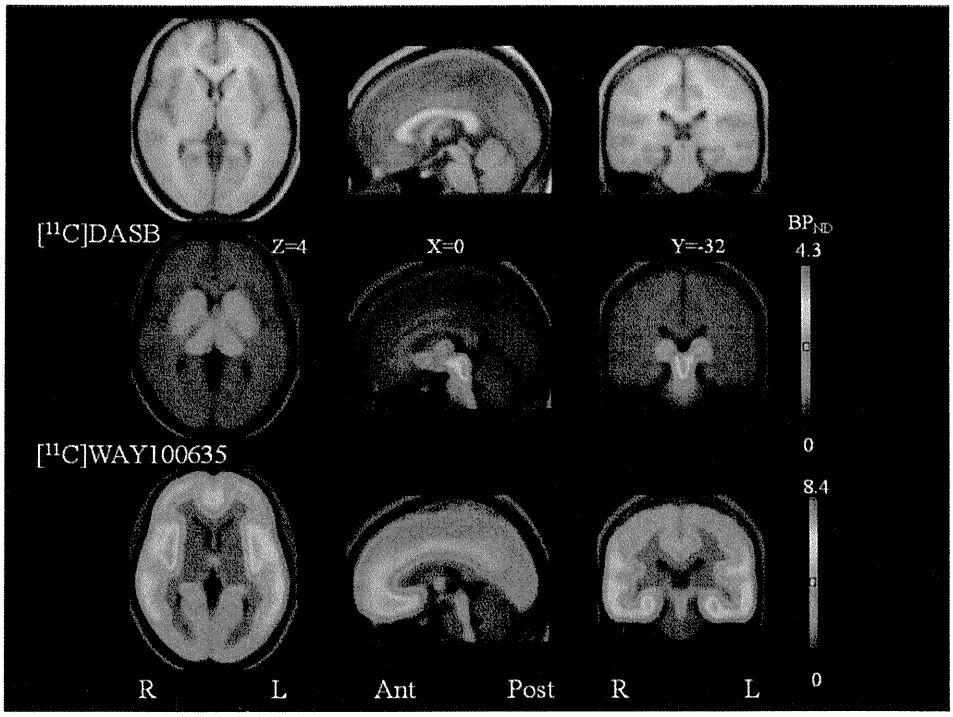

Fig. 2. Averaged images of MRI, [^{11}C]DASB image fused with MRI, and [^{11}C]WAY100635 image fused with MRI for all subjects. In left to right columns, transaxial, saggital, and coronal planes of the brain are displayed. X = 0 mm, Y = −32 mm, and Z = 4 mm indicate the coordinates of the three planes in the MNI template brain. R represents right; L, left. Ant indicates anterior; Post, posterior.

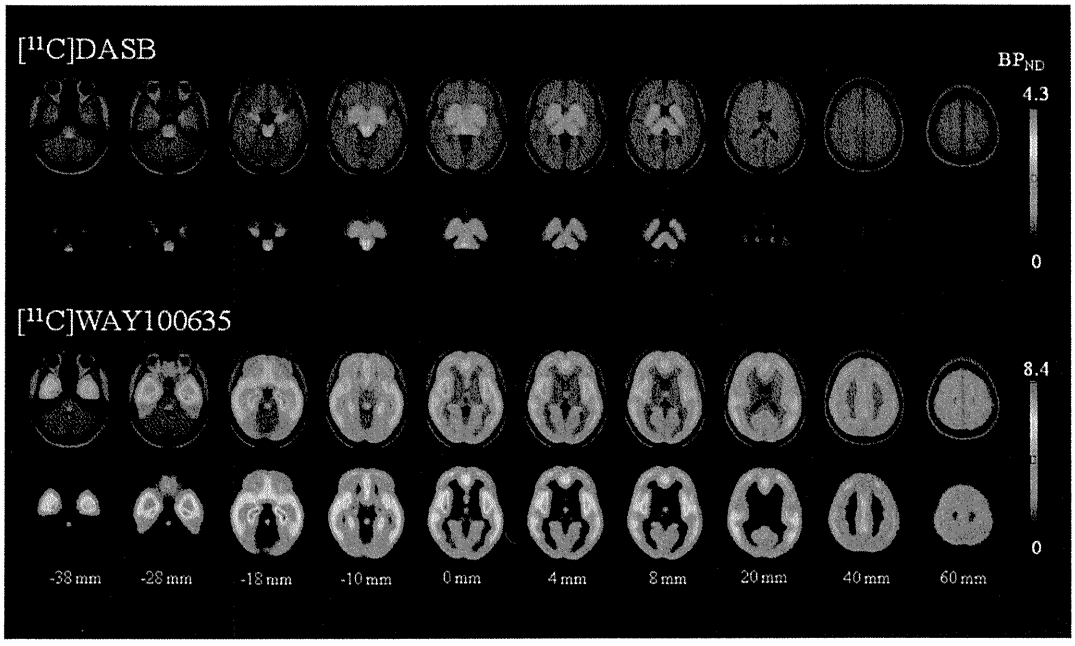

Fig. 3. Averaged BP_{ND} images with anatomical standardization of both radiotracers (axial planes). From the top row to the bottom: fused [^{11}C]WAY100635 and MRI, only [^{11}C]WAY100635, fused [^{11}C]DASB and MRI, only [^{11}C]DASB. In left to right columns: from ventral to dorsal planes of transverse images. L denotes left side of the brain; R denotes right side. Color bar indicates the value of BP_{ND}.

TABLE II. BPND values for each VOI

Region	[^{11}C]DASB			[^{11}C]WAY100635				
	Total	Right	Left	Total	Right	Left	r	P
Dorsal raphe nucleus	3.10 ± 0.97			2.17 ± 0.54			−0.191	0.464
Striatum	1.42 ± 0.28	1.40 ± 0.27	1.43 ± 0.30	1.42 ± 0.39	1.23 ± 0.38	1.58 ± 0.53	−0.333	0.192
Putamen	1.46 ± 0.29	1.45 ± 0.28	1.47 ± 0.30	1.72 ± 0.47	1.48 ± 0.48	1.94 ± 0.66	−0.368	0.146
Caudate head	1.25 ± 0.30	1.20 ± 0.28	1.29 ± 0.35	0.32 ± 0.23	0.29 ± 0.24	0.34 ± 0.25	0.208	0.423
Globus Pallidus	1.15 ± 0.36	1.14 ± 0.48	1.15 ± 0.31	0.35 ± 0.20	0.30 ± 0.22	0.40 ± 0.24	−0.446	0.073
Thalamus	1.88 ± 0.48	1.89 ± 0.53	1.87 ± 0.44	0.95 ± 0.27	1.03 ± 0.33	0.87 ± 0.26	−0.210	0.420
Anterior nucleus	1.93 ± 0.48	2.01 ± 0.57	1.84 ± 0.41	1.38 ± 0.41	1.37 ± 0.60	1.38 ± 0.34	−0.407	0.105
Dorsomedial nucleus	2.01 ± 0.51	2.08 ± 0.55	1.93 ± 0.50	1.23 ± 0.45	1.30 ± 0.55	1.16 ± 0.51	−0.328	0.199
Pulvinar	2.18 ± 0.73	2.03 ± 0.71	2.31 ± 0.79	0.89 ± 0.41	1.02 ± 0.43	0.77 ± 0.51	−0.079	0.762
Hippocampal complex	0.83 ± 0.18	0.83 ± 0.18	0.82 ± 0.19	6.30 ± 0.97	6.27 ± 1.03	6.33 ± 0.95	−0.306	0.232
Uncus	1.20 ± 0.27	1.18 ± 0.26	1.23 ± 0.29	5.78 ± 1.05	5.90 ± 1.10	5.66 ± 1.06	−0.268	0.297
Hippocampus	0.61 ± 0.18	0.58 ± 0.22	0.65 ± 0.17	7.01 ± 1.34	7.34 ± 1.55	6.71 ± 1.36	−0.226	0.383
Parahippocampus	0.52 ± 0.12	0.54 ± 0.13	0.51 ± 0.13	6.61 ± 1.03	6.36 ± 1.10	6.82 ± 1.11	−0.322	0.208
Insula	0.70 ± 0.17	0.75 ± 0.19	0.65 ± 0.15	6.65 ± 1.13	6.64 ± 1.14	6.67 ± 1.20	*−0.506	0.038
Anterior cingulate	0.45 ± 0.09	0.42 ± 0.11	0.47 ± 0.10	5.39 ± 0.83	5.46 ± 0.93	5.33 ± 0.90	*−0.539	0.026
Posterior cingulate	0.35 ± 0.07	0.37 ± 0.07	0.33 ± 0.10	4.76 ± 0.69	4.91 ± 0.73	4.57 ± 0.81	*−0.484	0.049
Base side of frontal cortex	0.21 ± 0.07	0.22 ± 0.08	0.20 ± 0.06	4.45 ± 0.76	4.54 ± 0.80	4.36 ± 0.75	*−0.539	0.026
Frontal convexity	0.20 ± 0.06	0.20 ± 0.06	0.19 ± 0.06	4.55 ± 0.82	4.53 ± 0.78	4.56 ± 0.87	−0.464	0.061
Lateral temporal	0.25 ± 0.05	0.26 ± 0.06	0.23 ± 0.05	5.73 ± 0.86	5.70 ± 0.86	5.76 ± 0.87	*−0.603	0.010
Occipital cuneus	0.39 ± 0.10	0.38 ± 0.11	0.40 ± 0.11	2.59 ± 0.51	2.55 ± 0.56	2.62 ± 0.51	−0.433	0.083
Parietal	0.12 ± 0.04	0.13 ± 0.04	0.12 ± 0.04	4.54 ± 0.71	4.61 ± 0.73	4.46 ± 0.74	*−0.718	0.001

r indicates Pearson's correlation coefficients between total BPND of [^{11}C]DASB and that of [^{11}C]WAY100635 for each VOI.
*Indicates $P < 0.05$.

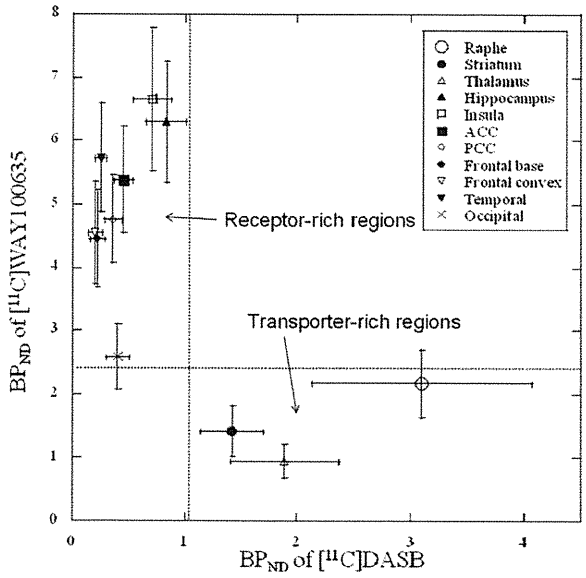

Fig. 4. Relationships between mean BP_{ND} values of [^{11}C]DASB and those of [^{11}C]WAY100635. The error bars indicate standard deviation.

indicating no apparent laterality in the distribution of 5-HTT and 5-HT_{1A} (paired t-test, data not shown). Moreover, no significant correlation between age and the binding of 5-HTT and 5-HT_{1A} was found in any of the brain regions within the age range (20–40 yr) of our sample (Pearson's correlation coefficient, $P > 0.05$, data not shown). In addition, with regard to the intraindividual relationship between the binding of both [^{11}C]DASB and [^{11}C]WAY100635 in the same region of the brain, significant negative correlations were observed in the anterior and posterior cingulate, insula, basal side of the frontal cortex, lateral temporal cortex, and parietal cortex (Table II and Fig. 5), whereas no significant positive correlation was observed.

DISCUSSION

We constructed a database of 5-HTT and 5-HT_{1A} serotonergic function by using parametric images generated by the anatomic standardization of the brains of 17 healthy young men. Anatomical standardization enables visualization of the entire neuroanatomy along the same coordinates with the help of multiple radiotracers that permit inter- and intrasubject comparisons. In the current study, the distributions of the two serotonergic markers differed. In addition, an exploratory study revealed significant inverse linear correlations between BP_{ND} of presynaptic 5-HTT and that of postsynaptic 5-HT_{1A} receptor binding in certain areas of the brain, such as the frontal, temporal, and parietal cortices; insula; and anterior and posterior cingulate.

Overall, the distribution patterns of 5-HTT and 5-HT_{1A} binding in the human brain were in accordance with those observed in previous human PET and postmortem studies (Brust et al., 2006; Drevets et al., 2007; Hall et al., 1997; Hoyer et al., 1986; Ito et al., 1999; Kish et al., 2005; Laruelle et al., 1988; Pazos et al., 1987; Rabiner et al., 2002; Savitz et al., 2009; Stockmeier, 2003; Varnas et al., 2004).

Localization of 5-HTT and 5-HT_{1A} in respective regions of the brain

In general, distributions in 5-HTT and 5-HT_{1A} receptors are quite different, and can be categorized into two groups, 5-HTT-rich regions and 5-HT_{1A} receptor-rich regions (Fig. 4). In 5-HT_{1A} receptor-rich regions such as the cerebral cortex and limbic

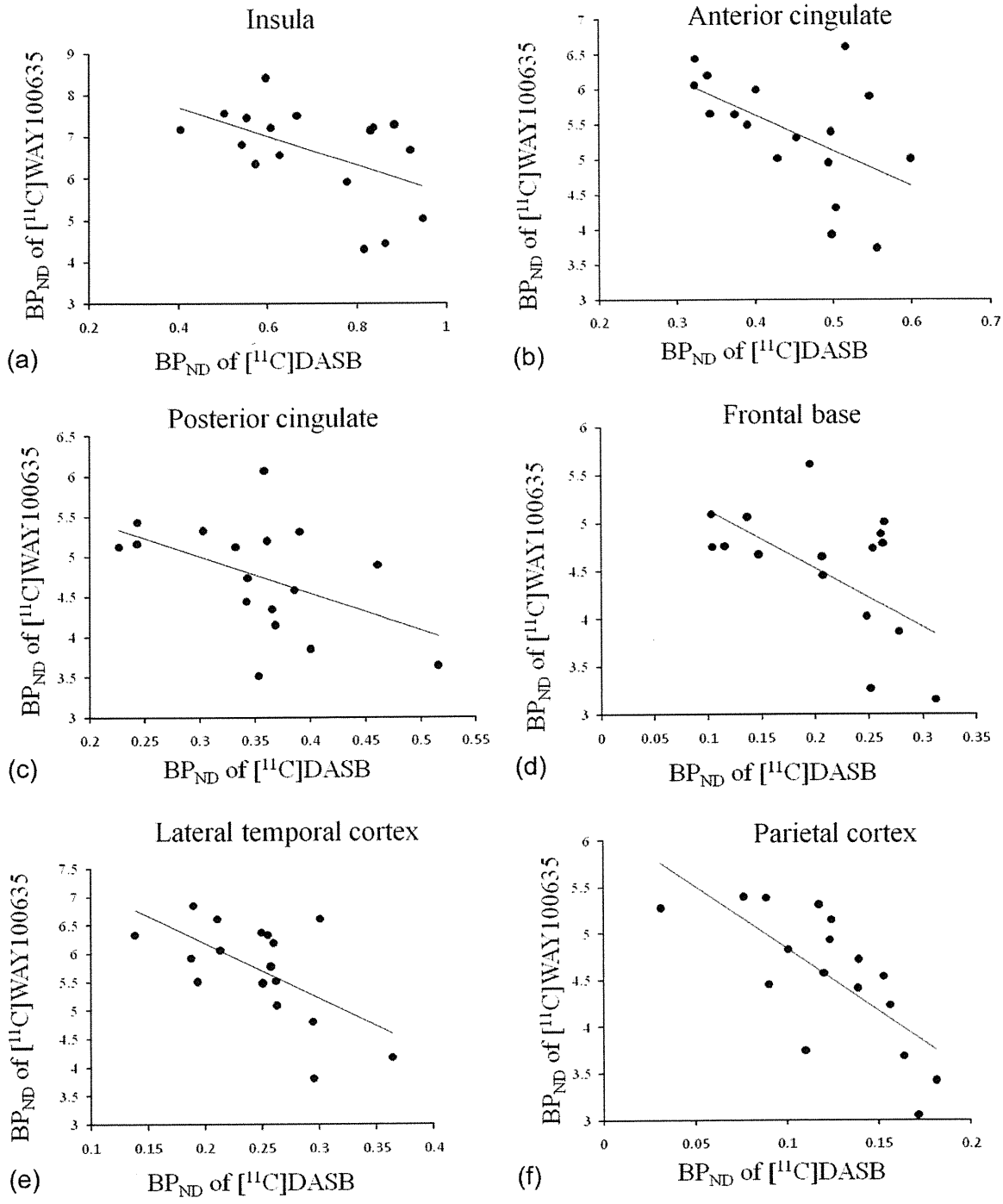

Fig. 5. Areas showing significant correlations of BP_{ND} values between [^{11}C]DASB and [^{11}C]WAY100635 in intrasubject comparisons. (a) insula, (b) anterior cingulate, (c) posterior cingulate, (d) base side of frontal cortex, (e) lateral temporal cortex, (f) parietal cortex.

regions, they tend to positively correlate with each other except the occipital cortex. This finding could reflect innervation of serotonergic fibers in those regions.

5-HTT-rich region

Brain stem. High binding to 5-HTT was observed in large areas of the midbrain, and it continuously

extended to the thalamus; this finding indicated rich distribution in these regions. In contrast, moderate binding to 5-HT_{1A} receptors was observed only in the dorsal and medial raphe, with this distribution indicating that 5-HT_{1A} receptor exists only in these regions of the midbrain (the sagittal section, middle column in the bottom row in Figure 2; the transverse sections, the first to fourth columns in the second row from the bottom; further, refer to the volume of interest 6 in Figure 1, which represents the raphe nuclei). These distribution patterns of 5-HTT and 5-HT_{1A} were consistent with those observed in previous human postmortem autoradiography studies (Hall et al., 1997; Varnas et al., 2004). In the present study, however, 5-HT_{1A} binding was not very high as compared with that in other areas (Table II). For example, the mean BP_{ND} value in the dorsal raphe was approximately one-third of that in the hippocampus, which exhibited the highest value of all regions examined. Further, in a detailed human autoradiography study with [^{3}H]WAY100635, binding to the dorsal raphe was highest (140 pmol/g tissue), followed by the hippocampus (123 pmol/g tissue). However, this discrepancy may be a result of the limited spatial resolution of the PET scanner, resulting in excessive spillover from the raphe and other small structures.

Subcortical regions. In the striatum (putamen and caudate) and globus pallidus, relatively high levels of binding to 5-HTT were observed. In contrast, 5-HT_{1A} receptor binding was very low or absent in the caudate nucleus and globus pallidus, while a low level of binding was found in the putamen. However, postmortem autoradiography studies showed very low levels of binding in the putamen, similar to those in the caudate and globus pallidus (Hall et al., 1997; Varnas et al., 2004); the high BP_{ND} values in the putamen may be attributed to spillover from the insula, which exhibits a very high level of 5-HT_{1A} binding.

The level of 5-HTT binding in the thalamus was the second highest among all brain regions, after the dorsal raphe nucleus; further, there was no marked difference in 5-HTT distribution among the subregions of the thalamus. These findings were similar to those of a previous human postmortem study (Varnas et al., 2004). On the other hand, the level of binding to the 5-HT_{1A} receptor was very low in the thalamus, although a little binding was observed in its medial parts regions (Table II and Figs. 2–4); this finding was similar to those of previous autoradiography studies showing much less or no binding in these regions (Hall et al., 1997; Varnas et al., 2004).

5-HT_{1A} receptor-rich region

Cerebral neocortex. Relatively high binding to 5-HT_{1A} and low binding to 5-HTT were observed in the neocortical regions. The 5-HT_{1A} receptor was widely distributed in the cerebral cortex but sparsely in the occipital cortex. The distribution of 5-HTT was very low in the neocortical regions as compared with other brain regions, but was found to be homogeneous among the cortical regions (Figs. 2–4, Table II). These findings were consistent with those of previous postmortem autoradiography studies (Hall et al., 1997; Laruelle et al., 1988; Varnas et al., 2004).

Limbic regions. In the hippocampal regions that include the parahippocampus, hippocampus, and uncus (amygdala), highest binding to 5-HT_{1A} and moderate binding to 5-HTT were observed (Figs. 2–4, Table II). Postmortem autoradiography studies in humans revealed that the highest binding to 5-HT_{1A} was observed particularly over the CA1 field in the hippocampus (Hall et al., 1997; Varnas et al., 2004). In contrast, binding to 5-HTT was higher in the uncus as compared to other hippocampal regions, a finding in agreement with a previous postmortem study (Varnas et al., 2004).

Within the cingulate cortex, both 5-HTT and 5-HT_{1A} binding can be described in descending order as follows: ventral (subcallosal) cingulate > anterior cingulate > posterior cingulate (Table II and Figs 2 and 3). In particular, the ventral cingulate is thought to be involved in the regulation of emotions and has been repeatedly reported to be associated with depression (Drevets et al., 2008; Seminowicz et al., 2004).

Very high 5-HT_{1A} binding and intermediate 5-HTT binding were observed in the insula. These distributions are in accordance with those found in previous human postmortem autoradiography studies (Varnas et al., 2004), although BP_{ND} values in the insula can be affected by spillover from the striatum, which exhibits high levels of 5-HTT binding.

Our findings together suggest that the limbic regions, including the hippocampal area, cingulate cortex, and insula, are relatively rich in serotonergic innervation. Thus, serotonergic transmission in these regions might play a pivotal role in modulating emotion and cognition.

Intraindividual relationship between the binding of both [^{11}C]DASB and [^{11}C]WAY100635 in the same region of the brain

With respect to the intraindividual relationship between regional 5-HTT and 5-HT_{1A} distribution, we found significant negative linear correlations between the binding of [^{11}C]DASB and [^{11}C]WAY100635 in the insula; anterior and posterior cingulate; and lateral temporal, frontal base, and parietal cortices. This result suggests that serotonergic transmission might be modulated by a cooperative relationship between 5-HTT and 5-HT_{1A}.

There have been only a few reports on pre- and postsynaptic serotonergic functions in individuals. In a study of 12 men, Lundberg et al. (2007) showed a positive linear correlation between 5-HTT and 5-HT_{1A} binding in the raphe nuclei and hippocampal complex using [^{11}C]MADAM and [^{11}C]WAY100635, respectively; however, a positive linear correlation was not observed in the frontal cortex. Another study that examined gender differences in binding using [^{11}C]MADAM and [^{11}C]WAY100635 also reported an interrelationship between 5-HTT and 5-HT_{1A} receptors (Jovanovic et al., 2008). They found a significant positive correlation between BP_{ND} of 5-HTT and 5-HT_{1A} receptors in the hippocampus of eight women, whereas no significant correlation was observed in seven men. The discrepancy between their results and ours could be attributed to the use of different 5-HTT radiotracers, sample size, and subjects' background. In particular, the age range of subjects in the study by Lundberg et al. was wider than ours, and different degrees of atrophy can cause positive correlation in BP_{ND} between 5-HTT and 5-HT_{1A} receptor. This is because older subjects are likely to have more brain atrophy, because of which both BP_{ND} values are lower than those of young subjects. Our results suggest that subjects exhibiting higher 5-HTT binding are likely to have less 5-HT_{1A} receptor binding and vice versa. One possible interpretation of this inter-subject difference is that individuals with higher 5-HT synthesis and release show a decrease in the 5-HT_{1A} receptor function to dampen the transmission at the postsynaptic site and an increase in 5-HTT function in order to reuptake more 5-HT at the presynaptic site, whereas individuals with lower 5-HT synthesis and release show an increase in the 5-HT_{1A} receptor function and a decrease in 5-HTT function to reuptake less 5-HT; that is, pre- and postsynaptic 5-HT functions are modulated cooperatively to compensate the overall 5-HT transmission. However, these studies were done under resting condition, and therefore challenge study designs using drugs or stress may help to better understand the relationship between pre- and postsynaptic functions.

Limitation

There are several limitations to the current study. First, the two PET studies were not always performed on the same day. Good reproducibility for both ligands (Kim et al., 2006; Rabiner et al., 2002), however, has been demonstrated, and it has been shown that the endogenous 5-HT level has no direct effect on binding (Rabiner et al., 2002; Talbot et al., 2005); hence, it is unlikely that the endogenous level affected the results. Second, the sample size was small, especially for a correlation study between pre- and postsynaptic functions, and our study should necessarily be regarded as a preliminary one. Third, we focused only on 5-HTT and 5-HT_{1A} receptors because they reportedly play pivotal roles in serotonergic functions. However, there are more than 10 receptor systems in the brain that affect serotonergic transmission. In addition, monoamine oxidase as well as 5-HTT are known to control the 5-HT concentration in the synapse (Nestler et al., 2008). Finally, the current study includes only young men, and we should expand it to women and individuals of a wider range of ages. Such a database will be helpful even for clinical studies on depression and anxiety disorders, since these disorders are known to show different prevalence and clinical features depending on gender and age (Fernandez et al., 1995; Gorman, 2006; Pigott, 1999). The physiological differences in the 5-HT system based on gender and age might explain the characteristics of depression and anxiety disorders.

In summary, we constructed a normal database to elucidate regional distributions of 5-HT_{1A} and 5-HTT binding. The neuroanatomy of the 5-HT_{1A} and 5-HTT serotonergic systems was discussed mostly by comparing our findings with those of previous postmortem studies. Furthermore, we explored the linear negative correlation between pre- and postsynaptic functions in certain parts of the brain. The results obtained indicate the involvement of a cooperative or complementary process in serotonergic transmission. Further studies are required to elucidate the modulation of 5-HT transmission in neuropsychiatric disorders and to clarify the various serotonergic systems involving pre- and postsynaptic functions in different regions of the brain.

ACKNOWLEDGMENTS

The authors thank Mr. Katuyuki Tanimoto, Mr. Takahiro Shiraishi, and Mr. Akira Ando for their assistance in performing PET examinations at the National Institute of Radiological Sciences. The authors are also grateful to Ms. Yoshiko Fukushima for the help as a clinical research coordinator.

REFERENCES

Brust P, Hesse S, Muller U, Szabo Z. 2006. Neuroimaging of the serotonin transporter. Curr Psychiatry Rev 2:111–149.
Cooper JR, Bloom FE, Roth RH. 2002. The biochemical basis of neuropharmacology, 8th ed. New York, USA: Oxford University Press.
Diksic M, Young SN. 2001. Study of the brain serotonergic system with labeled alpha-methyl-L-tryptophan. J Neurochem 78:1185–1200.
Drevets WC, Savitz J, Trimble M. 2008. The subgenual anterior cingulate cortex in mood disorders. CNS Spectr 13:663–681.
Drevets WC, Thase ME, Moses-Kolko EL, Price J, Frank E, Kupfer DJ, Mathis C. 2007. Serotonin-1A receptor imaging in recurrent depression: replication and literature review. Nucl Med Biol 34:865–877.
Fernandez F, Levy JK, Lachar BL, Small GW. 1995. The management of depression and anxiety in the elderly. J Clin Psychiatry 56(Suppl 2):20–29.
Gorman JM. 2006. Gender differences in depression and response to psychotropic medication. Gend Med 3:93–109.

Gunn RN, Lammertsma AA, Hume SP, Cunningham VJ. 1997. Parametric imaging of ligand-receptor binding in PET using a simplified reference region model. Neuroimage 6:279–287.

Gunn RN, Sargent PA, Bench CJ, Rabiner EA, Osman S, Pike VW, Hume SP, Grasby PM, Lammertsma AA. 1998. Tracer kinetic modeling of the 5-HT1A receptor ligand [carbonyl-^{11}C]WAY-100635 for PET. Neuroimage 8:426–440.

Hall H, Lundkvist C, Halldin C, Farde L, Pike VW, McCarron JA, Fletcher A, Cliffe IA, Barf T, Wikstrom H, Sedvall G. 1997. Autoradiographic localization of 5-HT_{1A} receptors in the post-mortem human brain using [^{3}H]WAY-100635 and [^{11}C]way-100635. Brain Res 745:96–108.

Hoyer D, Hannon JP, Martin GR. 2002. Molecular, pharmacological and functional diversity of 5-HT receptors. Pharmacol Biochem Behav 71:533–554.

Hoyer D, Pazos A, Probst A, Palacios JM. 1986. Serotonin receptors in the human brain. I. Characterization and autoradiographic localization of 5-HT_{1A} recognition sites. Apparent absence of 5-HT_{1B} recognition sites. Brain Res 376:85–96.

Ichise M, Liow JS, Lu JQ, Takano A, Model K, Toyama H, Suhara T, Suzuki K, Innis RB, Carson RE. 2003. Linearized reference tissue parametric imaging methods: application to [^{11}C]DASB positron emission tomography studies of the serotonin transporter in human brain. J Cereb Blood Flow Metab 23:1096–1112.

Ichise M, Toyama H, Innis RB, Carson RE. 2002. Strategies to improve neuroreceptor parameter estimation by linear regression analysis. J Cereb Blood Flow Metab 22:1271–1281.

Innis RB, Cunningham VJ, Delforge J, Fujita M, Gjedde A, Gunn RN, Holden J, Houle S, Huang SC, Ichise M, Iida H, Ito H, Kimura Y, Koeppe RA, Knudsen GM, Knuuti J, Lammertsma AA, Laruelle M, Logan J, Maguire RP, Mintun MA, Morris ED, Parsey R, Price JC, Slifstein M, Sossi V, Suhara T, Votaw JR, Wong DF, Carson RE. 2007. Consensus nomenclature for in vivo imaging of reversibly binding radioligands. J Cereb Blood Flow Metab 27:1533–1539.

Ito H, Halldin C, Farde L. 1999. Localization of 5-HT_{1A} receptors in the living human brain using [carbonyl-^{11}C]WAY-100635: PET with anatomic standardization technique. J Nucl Med 40:102–109.

Ito H, Takahashi H, Arakawa R, Takano H, Suhara T. 2008. Normal database of dopaminergic neurotransmission system in human brain measured by positron emission tomography. Neuroimage 39:555–565.

Jovanovic H, Lundberg J, Karlsson P, Cerin A, Saijo T, Varrone A, Halldin C, Nordstrrom A-L. 2008. Sex differences in the serotonin 1A receptor and serotonin transporter binding in the human brain measured by PET. Neuroimage 39:1408–1419.

Kim JS, Ichise M, Sangare J, Innis RB. 2006. PET imaging of serotonin transporters with [^{11}C]DASB: test-retest reproducibility using a multilinear reference tissue parametric imaging method. J Nucl Med 47:208–214.

Kish SJ, Furukawa Y, Chang LJ, Tong J, Ginovart N, Wilson A, Houle S, Meyer JH. 2005. Regional distribution of serotonin transporter protein in postmortem human brain: is the cerebellum a SERT-free brain region? Nucl Med Biol 32:123–128.

Kitson SL. 2007. 5-hydroxytryptamine (5-HT) receptor ligands. Curr Pharm Des 13:2621–2637.

Kumar JSD, Mann JJ. 2007. PET tracers for 5-HT(1A) receptors and uses thereof. Drug Discov Today 12:748–756.

Lammertsma AA, Hume SP. 1996. Simplified reference tissue model for PET receptor studies. Neuroimage 4:153–158.

Laruelle M, Vanisberg MA, Maloteaux JM. 1988. Regional and subcellular localization in human brain of [^{3}H]paroxetine binding, a marker of serotonin uptake sites. Biol Psychiatry 24:299–309.

Lundberg J, Borg J, Halldin C, Farde L. 2007. A PET study on regional coexpression of 5-HT_{1A} receptors and 5-HTT in the human brain. Psychopharmacology 195:425–433.

Lundquist P, Blomquist G, Hartvig P, Hagberg GE, Torstenson R, Hammarlund-Udenaes M, Langstrom B. 2006. Validation studies on the 5-hydroxy-L-[beta-^{11}C]-tryptophan/PET method for probing the decarboxylase step in serotonin synthesis. Synapse 59:521–531.

Marner L, Gillings N, Comley RA, Baare WF, Rabiner EA, Wilson AA, Houle S, Hasselbalch SG, Svarer C, Gunn RN, Laruelle M, Knudsen GM. 2009. Kinetic modeling of ^{11}C-SB207145 binding to 5-HT_4 receptors in the human brain in vivo. J Nucl Med 50:900–908.

Meyer JH. 2007. Imaging the serotonin transporter during major depressive disorder and antidepressant treatment. J Psychiatry Neurosci 32:86–102.

Moresco RM, Matarrese M, Fazio F. 2006. PET and SPET molecular imaging: Focus on serotonin system. Curr Top Med Chem 6:2027–2034.

Nestler E, Hyman S, Malenka R. 2008. Molecular neuropharmacology: A foundation for clinical neuroscience, 2nd ed. New York, USA: McGraw-Hill Professional.

Pazos A, Probst A, Palacios JM. 1987. Serotonin receptors in the human brain. III. Autoradiographic mapping of serotonin-1 receptors. Neuroscience 21:97–122.

Pigott TA. 1999. Gender differences in the epidemiology and treatment of anxiety disorders. J Clin Psychiatry 60(Suppl 18):4–15.

Rabiner EA, Messa C, Sargent PA, Husted-Kjaer K, Montgomery A, Lawrence AD, Bench CJ, Gunn RN, Cowen P, Grasby PM. 2002. A database of [^{11}C]WAY-100635 binding to 5-HT_{1A} receptors in normal male volunteers: Normative data and relationship to methodological, demographic, physiological, and behavioral variables. Neuroimage 15:620–632.

Savitz J, Lucki I, Drevets WC. 2009. 5-HT_{1A} receptor function in major depressive disorder. Prog Neurobiol 88:17–31.

Seminowicz DA, Mayberg HS, McIntosh AR, Goldapple K, Kennedy S, Segal Z, Rafi-Tari S. 2004. Limbic-frontal circuitry in major depression: A path modeling metanalysis. Neuroimage 22:409–418.

Stockmeier CA. 2003. Involvement of serotonin in depression: Evidence from postmortem and imaging studies of serotonin receptors and the serotonin transporter. J Psychiatr Res 37:357–373.

Suhara T, Sudo Y, Yoshida K, Okubo Y, Fukuda H, Obata T, Yoshikawa K, Suzuki K, Sasaki Y. 1998. Lung as reservoir for antidepressants in pharmacokinetic drug interactions. Lancet 351:332–335.

Talbot PS, Frankle WG, Hwang DR, Huang Y, Suckow RF, Slifstein M, Abi-Dargham A, Laruelle M. 2005. Effects of reduced endogenous 5-HT on the in vivo binding of the serotonin transporter radioligand ^{11}C-DASB in healthy humans. Synapse 55:164–175.

Varnas K, Halldin C, Hall H. 2004. Autoradiographic distribution of serotonin transporters and receptor subtypes in human brain. Hum Brain Mapp 22:246–260.

Epilepsy Research (2011) xxx, xxx–xxx

ELSEVIER

journal homepage: www.elsevier.com/locate/epilepsyres

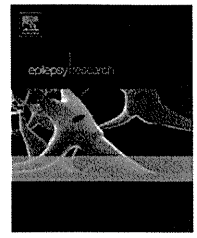

Abnormal mismatch negativity for pure-tone sounds in temporal lobe epilepsy

Miho Miyajima[a,b,*], **Katsuya Ohta**[a,c,d], **Keiko Hara**[b,d], **Hiroko Iino**[e], **Taketoshi Maehara**[f], **Minoru Hara**[b], **Masato Matsuura**[d], **Eisuke Matsushima**[a]

[a] *Section of Liaison Psychiatry and Palliative Medicine, Graduate School of Medical and Dental Sciences, Tokyo Medical and Dental University, Tokyo, Japan*
[b] *Hara Clinic, Kanagawa, Japan*
[c] *Onda-daini Hospital, Chiba, Japan*
[d] *Section of Life Sciences and Biofunctional Informatics, Graduate School of Health Care Sciences, Tokyo Medical and Dental University, Tokyo, Japan*
[e] *Department of Clinical Laboratory, The University of Tokyo Hospital, Tokyo, Japan*
[f] *Department of Neurosurgery, Tokyo Medical and Dental University, Tokyo, Japan*

Received 31 May 2010; received in revised form 8 January 2011; accepted 23 January 2011

KEYWORDS
Temporal lobe epilepsy (TLE);
Event-related potentials (ERPs);
Mismatch negativity (MMN);
Auditory processing;
Pre-attentive memory

Summary Auditory processing abnormalities in temporal lobe epilepsy (TLE) were assessed by investigating mismatch negativity (MMN) in a group of 20 TLE patients and 20 healthy control subjects. MMN is an event-related potential (ERP) component that reflects pre-attentive sensory memory function. A passive oddball paradigm using frequency changes in sinusoidal tones was employed to evoke MMN. MMN at frontocentral sites was enhanced in TLE patients relative to controls, while mismatch signals at mastoid sites (i.e., mismatch positivity; MMP) did not differ between the two groups. In the MMP temporal range, greater positivity at mastoid sites in response to standard stimuli was observed in TLE patients than in controls. Both MMN and MMP were significantly delayed in the TLE group. These findings demonstrate that TLE patients have impaired pre-attentive processing of pure-tone sounds. Enhanced frontocentral MMN may reflect hyperexcitability of the frontal lobes in compensation for dysfunction of the temporal lobes. Larger positivity at the mastoids in response to standard stimuli may be attributed to poor neuronal adaptation in the temporal lobe. Taken together, results suggest that evaluation of MMN/P is a useful physiological tool for identifying pre-attentive auditory memory dysfunction in TLE.

* Corresponding author at: Section of Liaison Psychiatry and Palliative Medicine, Graduate School of Medical and Dental Sciences, Tokyo Medical and Dental University, Tokyo 113-8519, Japan. Tel.: +81 358035859; fax: +81 358030217.
E-mail address: miholppm@tmd.ac.jp (M. Miyajima).

0920-1211/$ – see front matter © 2011 Elsevier B.V. All rights reserved.
doi:10.1016/j.eplepsyres.2011.01.009

Please cite this article in press as: Miyajima, M., et al., Abnormal mismatch negativity for pure-tone sounds in temporal lobe epilepsy. Epilepsy Res. (2011), doi:10.1016/j.eplepsyres.2011.01.009

Introduction

Temporal lobe epilepsy (TLE) is often associated with memory impairment due to damage in the hippocampus and surrounding structures (Dietl et al., 2008; McCagh et al., 2009). It has been repeatedly shown that both short-term and long-term memory are impaired in TLE (Butler and Zeman, 2008; McCagh et al., 2009). However, little is known concerning dysfunction in initial sensory memory encoding in TLE.

Mismatch negativity (MMN) is an early auditory event-related potential (ERP) elicited when infrequent (''deviant'') sounds occur in a sequence of repetitive (''standard'') sounds (Näätänen et al., 1978). It has been proposed that MMN automatically arises if there is mismatch between the physical features of a deviant stimulus and a neuronal sensory-memory trace produced by repetitive standard stimuli (Näätänen et al., 1989). MMN is believed to reflect the earliest cortical event in the cognitive processing of auditory information (Pfefferbaum et al., 1995) and thus to be a part of auditory pre-attentive memory (Cowan et al., 1993). MMN can be elicited even in the absence of attention, and effects of motivation are minimal (Näätänen, 2000). MMN has therefore received considerable interest because of its potential application to clinical research, and has been studied in various populations including newborns (Stefanics et al., 2009) and children (Milovanov et al., 2009) as well as in disorders such as schizophrenia (Kasai et al., 2002; Salisbury et al., 2007) and Alzheimer's disease (Pekkonen et al., 2001). Focusing on pre-attentive processes may be the only means of assessing cognitive function in patients with advanced cognitive decay who are unable to perform traditional cognitive tasks.

To date, the extant literature evaluating MMN response in epilepsy patients is limited and discrepant, with some studies pointing to attenuated or delayed MMN, whereas others report enhanced MMN. For example, Lin et al. (2007) investigated the magnetic equivalent of mismatch negativity (MMNm) in intractable TLE patients using magnetoencephalography (MEG). Longer MMNm latencies were observed in patients than in healthy controls. The authors also evaluated inter-trial phase coherence as indexed by phase-locking factors using wavelet-based analyses. For patients who became seizure-free after removal of right temporal epileptic foci, phase-locking in response to deviant stimuli was enhanced and more strongly distributed in frontotemporal regions. Such findings suggest that successful surgery may improve auditory change detection. Borghetti et al. (2007) demonstrated similar improvements in drug-resistant epilepsy patients who underwent vagus nerve stimulation (VNS). Prior to VNS implantation, MMN latencies in some patients were abnormally late and attenuated relative to controls. After implantation, however, these patients exhibited a major reduction in MMN latency and increase in amplitude, suggesting a positive effect of VNS on pre-attentive processes.

In the pediatric field, MMN has been shown to be absent or prolonged for speech (but not tones) in patients with benign childhood epilepsy with centro-temporal spikes (BCECTS) (Boatman et al., 2008; Duman et al., 2008). Patients with BCECTS with atypical features and learning difficulties have also been shown to exhibit attenuated MMN amplitudes (Metz-Lutz and Filippini, 2006). Furthermore, Honbolygó et al. (2006) found that in Landau—Kleffner syndrome, MMN was obtained for phoneme differences but was absent for stress pattern differences.

In contrast to findings of attenuated MMN amplitudes and delayed latencies, Usui et al. (2009) observed distinctively large N100m signals, the magnetic counterpart of N1/N100, in autosomal-dominant lateral temporal lobe epilepsy with seizures provoked by auditory stimuli. Similarly, Gene-Cos et al. (2005) reported that MMN amplitudes tended to be larger in patients with epilepsy than in healthy controls. Furthermore, work from our own laboratory has shown extremely large MMN amplitudes in response to high-frequency deviants in a patient with frontal lobe epilepsy with seizures provoked by high-frequency auditory stimuli (Miyajima et al., 2009). One could hypothesize that the higher amplitudes observed in epileptic patients indicate increased activation of the same neuronal population as in controls, or that extra neuronal circuits are activated in epileptic patients (Myatchin et al., 2009).

Taken together, the existing literature provides discrepant accounts of how MMN is affected in epilepsy patients. Furthermore, most studies in adult epileptics have not focused on patients with specific types of epileptic syndromes or epileptogenic regions. To this end, the broad aim of the current study was to better characterize potential differences in cortical activation patterns between TLE patients and controls during pre-attentive auditory processing. Specifically, we employed a passive oddball task and evaluated whether frontal and mastoid mismatch components were equally affected by TLE. If a single auditory cortex generator is responsible for any potential abnormalities in TLE, we hypothesized that similar MMN changes should be expected across electrode locations, given that frontal and mastoid electrodes are approximately equidistant from Heschl's gyrus (Baldeweg et al., 2002).

In addition to characterizing MMN differences between TLE patients and controls, a secondary objective was to investigate whether MMN abnormalities, if present in TLE patients, were associated with epileptic seizures. Specifically, we evaluated whether mismatch components differed between patients who experienced at least one seizure in the months leading up to the experiment and patients who were seizure-free during the same time period.

Methods

Subjects

Twenty TLE patients (8 females and 12 males; mean age 33.9 ± 10.0 (SD) years) and 20 comparable healthy control subjects (10 females and 10 males; mean age 34.0 ± 7.8 years) participated in this study as volunteers.

Epilepsy patients were recruited from Tokyo Medical and Dental University Hospital and Hara Clinic, a specialized epilepsy clinic certified as a training facility by The Japan Epilepsy Society. All patients had partial seizures with features strongly suggestive of a TLE diagnosis, including simple partial seizures characterized by autonomic and/or psychic symptoms, certain phenomena such as olfactory and auditory sensations, and complex partial seizures beginning with motor arrest followed by oroalimentary automatism

Please cite this article in press as: Miyajima, M., et al., Abnormal mismatch negativity for pure-tone sounds in temporal lobe epilepsy. Epilepsy Res. (2011), doi:10.1016/j.eplepsyres.2011.01.009

Table 1 Clinical information for healthy controls and TLE patients.

Variables	Controls ($n=20$)			TLE patients ($n=20$)			
	Mean	(SD)	Range	Mean	(SD)	Range	
Age (years)	34.0	(7.8)	23–50	33.9	(10.0)	20–50	NS
Education (years)	16.6	(3.3)	12–22	14.5	(1.7)	12–16	NS
Gender (male/female)	10/10			12/8			
Duration of epilepsy (years)	NA			13.7	(9.8)	3–33	
Age of onset (years)	NA			20.1	(11.4)	0–45	
Side of epileptic focus (left/right/bilateral or undetermined)	NA			9/4/7			
Seizure status (intractable/remission)	NA			12/8			
Number of AED	NA			1.8	(1.0)	1–4	

AED, antiepileptic drug; NA, not applicable; NS, no significant difference.

(Commission on Classification and Terminology of the International League Against Epilepsy, 1989). Diagnoses were based on a combination of clinical symptoms, EEG, and structural/functional imaging data. Exclusion criteria for both groups included comorbid psychiatric disease, substance abuse or dependence, and reports of hearing or vision problems at the time of the experiment. Additional exclusion criteria for the control group included a history of psychiatric disease, history of traumatic brain injury with any known cognitive consequences or loss of consciousness, history of convulsions other than simple febrile seizures, and psychiatric disease or epileptic disorder in first-degree relatives.

Table 1 summarizes the subjects' clinical characteristics. Patients were divided into two subgroups, an intractable subgroup and a remission subgroup. The intractable subgroup experienced at least one seizure within a 20-month period prior to the experiment, while the remission subgroup was completely seizure-free during this time. All patients were treated with at least one anti-epileptic drug (AED), e.g., carbamazepine or phenytoin, for seizure control.

The study was approved by the Ethics Committee at Tokyo Medical and Dental University. Written informed consent was obtained from each participant after thoroughly describing the experiment.

Procedure

Subjects were presented with auditory stimulus sequences consisting of 600 standard stimuli and 150 deviant stimuli delivered in random order. Fifty deviant stimuli were presented to each subject in a single block, and each subject completed three blocks. The experimental conditions were designed to elicit MMN in response to changes in frequency of pure tones. To this end, stimuli consisted of pure tones presented for 100 ms each, with a rise/fall time of 5 ms and a stimulus onset asynchrony (SOA) of 500 ms. Standard stimuli (1000 Hz) comprised 80% of all trials, while deviant stimuli (1050 Hz) comprised 20%. The standard pure tone frequency of 1000 Hz is commonly used in psychoacoustic and electrophysiological studies, and was chosen because it does not directly correspond to the fundamental of any musical note. Stimuli were delivered binaurally via earphones at 90 dB as subjects watched a silent film while seated and were instructed to ignore auditory stimuli.

ERP recording

EEG was recorded using a portable bio-amplifier recording device (Polymate AP-1532 with silver/silver chloride electrodes, or Polymate AP-216 with active electrodes, TEAC Corporation, Japan) from the midline (Fz, Cz, Pz, and Oz) and bilateral mastoids. The tip of the nose served as the reference for all electrodes. Two electrodes were placed above the left eye and below the right eye to monitor the electrooculogram (EOG). Impedance between the electrodes and skin did not exceed 5 kΩ. The sampling rate was 1000 Hz for each channel and the recording bandwidth was between 0.05 Hz and 300 Hz.

Data analysis

Data analysis focused on a 600 ms time window ranging from 100 ms pre-stimulus to 500 ms post-stimulus onset. The pre-stimulus baseline was corrected separately for each channel according to the mean EEG amplitude over the 100 ms period. Averaging and artifact rejection were performed off-line. Trials with excessive movement activity or with EOG activity exceeding 100 μV peak-to-peak were excluded from analysis. Average waveforms were obtained separately for deviant and standard stimuli, with a minimum of 100 deviant trials for each subject.

Because MMN is known to show inverted polarity at mastoid locations, the term 'mismatch positivity' (MMP) has been adopted to describe the mismatch component at this location (Baldeweg et al., 1999). For this reason, we use the term MMP when describing mastoid findings, and MMN for findings at all other electrode locations.

Statistical analyses

The mean amplitudes of standard and deviant waveforms were defined as the average amplitude for each waveform 100–250 ms post-stimulus onset (the range in which MMN/P is typically found). MMN/P peak latency was defined as the latency of the peak showing maximal negativity/positivity 100–250 ms post-stimulus onset for the deviant – standard difference waveform.

Mean amplitudes for standard and deviant waveforms were first analyzed using three-way repeated-measures analyses of variance (ANOVA), with separate ANOVAs conducted for sites with negative and positive polarity. For both ANOVAs, factors included the between-subjects factor GROUP (TLE and control), and two within-subject factors STIMULUS (standard and deviant) and SITE (for sites with negative polarity: Fz and Cz; for sites with positive polarity: left and right mastoid). Additional two-way ANOVAs with one between-subject factor GROUP (TLE and control), and one within-subject factor SITE (for sites with negative polarity: Fz and Cz; for sites with positive polarity: left and right mastoid) followed separately for standard and deviant waveforms.

MMN/P peak latencies based on the difference waveform were examined using two-way repeated-measures ANOVAs with one between-subject factor GROUP (TLE and control), and one within-

Please cite this article in press as: Miyajima, M., et al., Abnormal mismatch negativity for pure-tone sounds in temporal lobe epilepsy. Epilepsy Res. (2011), doi:10.1016/j.eplepsyres.2011.01.009

Table 2 Mean amplitudes of standard, deviant and difference (MMN) waveforms as well as MMN peak latencies in controls and TLE patients.

Variables	Site		Controls ($n=20$)		TLE patients ($n=20$)	
			Mean	(SD)	Mean	(SD)
Mean amplitude (μV)						
Standard	Frontocentral	Fz	0.17	(0.70)	0.17	(1.31)
		Cz	0.15	(0.69)	0.07	(1.12)
	Mastoid	L	−0.22	(0.66)	0.43	(0.56)
		R	−0.31	(0.67)	0.42	(0.59)
Deviant	Frontocentral	Fz	0.11	(0.73)	−0.56	(1.59)
		Cz	0.24	(1.07)	−0.55	(1.39)
	Mastoid	L	0.13	(0.60)	0.49	(0.98)
		R	0.16	(0.56)	0.45	(1.20)
MMN	Frontocentral	Fz	−0.05	(0.73)	−0.75	(0.84)
		Cz	−0.10	(1.19)	−0.64	(0.93)
	Mastoid	L	0.35	(0.51)	0.06	(0.91)
		R	0.47	(0.58)	0.02	(0.63)
Peak latency (ms)						
MMN	Frontocentral	Fz	133	(28)	179	(36)
		Cz	141	(42)	171	(41)
	Mastoid	L	145	(31)	157	(53)
		R	150	(33)	185	(39)

subject factor SITE (for sites with negative polarity: Fz and Cz; for sites with positive polarity: left and right mastoid).

Finally, to explore whether potential abnormalities in TLE patients were associated with epileptic seizures, the TLE group was divided into two subgroups, an intractable subgroup and a remission subgroup. Mean amplitudes for standard and deviant waveforms were first analyzed using three-way ANOVAs with one between-subjects factor SUBGROUP (intractable and remission), and two within-subject factors STIMULUS (standard and deviant) and SITE (for sites with negative polarity: Fz and Cz; for sites with positive polarity: left and right mastoid). When a three-way ANOVA yielded a significant interaction or trend for an interaction between factors, a two-way ANOVA was performed for the relevant factors. MMN/P peak latencies based on the difference waveform were examined using two-way repeated-measures ANOVAs with one between-subjects factor SUBGROUP (intractable and remission), and one within-subject factor SITE (for sites with negative polarity: Fz and Cz; for sites with positive polarity: left and right mastoid).

With respect to all analyses, statistics for sites showing a negative mismatch component were limited to Fz and Cz because MMN typically is largest at midline frontocentral sites. As anticipated, visual inspection of difference waveforms at Pz and Oz revealed small and obscure mismatch signals such that it was difficult to determine individual peaks. MMN typically reverses polarity at nose-referenced mastoid sites. To this end, evaluation of waveforms at mastoid sites enabled comparison of polarity with waveforms at Fz and Cz, providing additional assurance that the observed negativity at these sites was a "true" mismatch response (Näätänen et al., 2007).

Results

Fig. 1 presents grand-averaged ERP waveforms for standard and deviant stimuli in TLE patients and controls at Fz, Cz, and left and right mastoids, with associated mean amplitudes presented in Table 2. Although statistical analyses

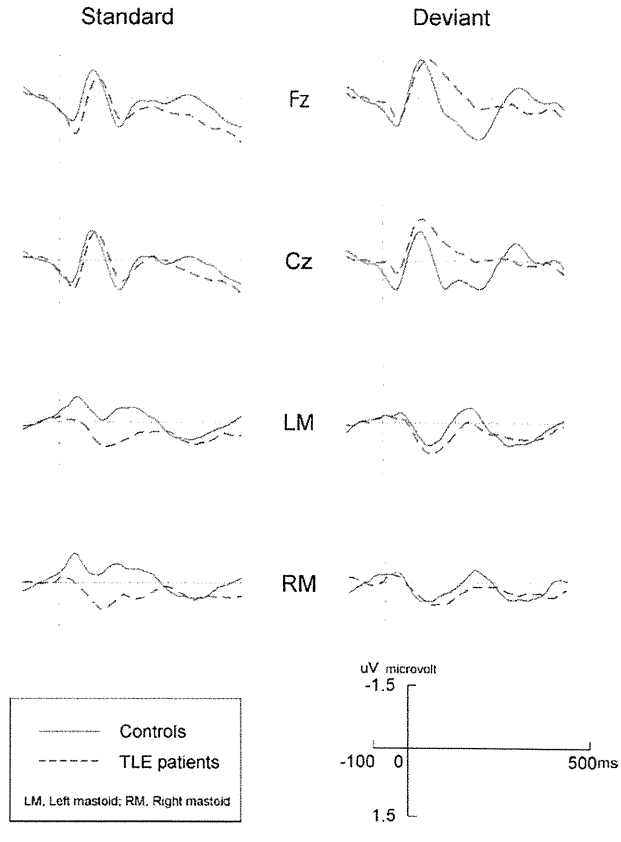

Figure 1 Comparison between grand-averaged ERPs for standard and deviant stimuli in controls and TLE patients. Solid line, control group; striped line, epilepsy group.

Please cite this article in press as: Miyajima, M., et al., Abnormal mismatch negativity for pure-tone sounds in temporal lobe epilepsy. Epilepsy Res. (2011), doi:10.1016/j.eplepsyres.2011.01.009

Table 3 Mean amplitudes of standard deviant and difference (MMN) waveforms as well as MMN peak latencies in TLE intractable and remission subgroups.

Variables	Site		Intractable ($n=12$)		Remission ($n=8$)	
			Mean	(SD)	Mean	(SD)
Mean amplitude (μV)						
Standard	Frontocentral	Fz	0.23	(0.64)	0.08	(0.61)
		Cz	0.12	(1.46)	−0.01	(0.53)
	Mastoid	L	0.45	(0.68)	0.40	(0.36)
		R	0.43	(0.70)	0.43	(0.39)
Deviant	Frontocentral	Fz	−0.60	(1.91)	−0.51	(1.06)
		Cz	−0.66	(1.50)	−0.38	(1.29)
	Mastoid	L	0.36	(1.09)	0.70	(0.82)
		R	0.36	(1.06)	0.57	(0.53)
MMN	Frontocentral	Fz	−0.82	(0.84)	−0.63	(0.87)
		Cz	−0.78	(0.85)	−0.38	(1.03)
	Mastoid	L	−0.10	(0.96)	0.09	(0.90)
		R	−0.06	(0.73)	0.02	(0.58)
Peak latency (ms)						
MMN	Frontocentral	Fz	183	(34)	149	(72)
		Cz	172	(43)	148	(73)
	Mastoid	L	165	(64)	126	(59)
		R	193	(45)	147	(64)

for mean amplitude were performed based upon standard and deviant waveforms, we also present grand-averaged MMN/P waveforms (i.e., difference waveforms) in Fig. 2 for ease of comparing mismatch signals across groups. For the same reason, MMN/P mean amplitudes also are presented in Table 2, with mean amplitude defined as the average amplitude of the deviant − standard difference waveform 100–250 ms post-stimulus onset. Peak latencies for the difference waveform are also reported in Table 2. Finally, Table 3 presents data relevant to the TLE subgroup analysis, including mean amplitudes of standard, deviant and difference (MMN/P) waveforms, as well as peak latencies of the MMN/P waveform.

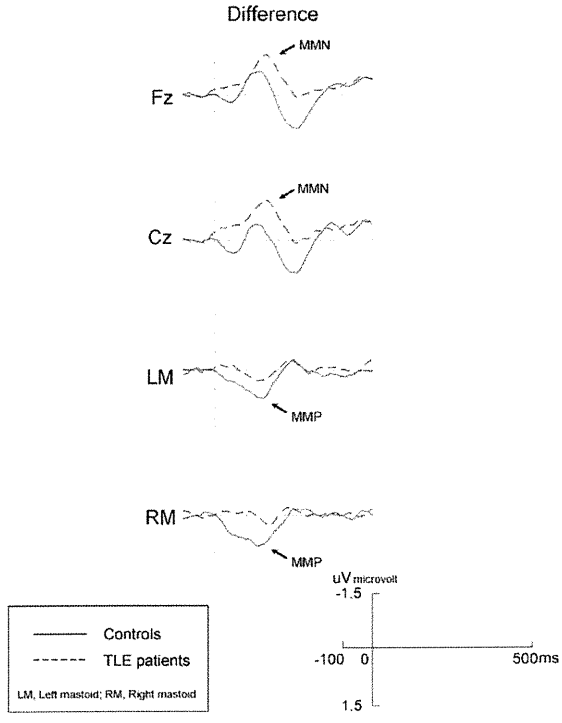

Figure 2 Deviant minus standard difference waveforms in controls and TLE patients. Solid line, control group; striped line, epilepsy group.

Frontocentral sites

A 2 (GROUP: TLE vs. control) × 2 (STIMULUS: standard vs. deviant) × 2 (SITE: Fz vs. Cz) repeated-measures ANOVA examining mean amplitudes for standard and deviant stimuli in the range of 100–250 ms revealed a significant main effect of STIMULUS [$F(1, 38)=5.05$, $p<0.05$], such that deviant amplitudes were greater than standard amplitudes. A significant interaction between STIMULUS and GROUP was also found [$F(1, 38)=5.74$, $p<0.05$], indicating that the difference between deviant and standard amplitudes in TLE patients was greater than that in controls. Stated another way, MMN was enhanced in TLE patients relative to controls (see Figs. 1 and 2 and Table 2). Separate 2 (SITE: Fz vs. Cz) × 2 (GROUP: TLE vs. control) repeated-measures ANOVAs for deviant and standard mean amplitudes showed no significant main effects or interactions. Additionally, visual inspection of waveforms revealed that deviant waveforms in TLE patients were still negative at a latency of 200 ms, whereas in controls deviant waveforms shifted from negative to positive around 150 ms, effectively leading to prolonged MMN duration in TLE patients (see Fig. 1 and Table 2).

Please cite this article in press as: Miyajima, M., et al., Abnormal mismatch negativity for pure-tone sounds in temporal lobe epilepsy. Epilepsy Res. (2011), doi:10.1016/j.eplepsyres.2011.01.009

With respect to MMN peak latency (based on the deviant − standard difference waveform), a two-way repeated measures ANOVA revealed a significant main effect of GROUP [$F(1, 38) = 12.45$, $p < 0.01$], such that MMN peak latency was delayed in patients compared with controls. No significant main effect of SITE or interaction between GROUP and SITE was observed.

Mastoid sites

A three-way repeated-measures ANOVA examining mean amplitudes for standard and deviant stimuli revealed significant main effects of both GROUP [$F(1, 38) = 7.14$, $p < 0.05$] and STIMULUS [$F(1, 38) = 5.08$, $p < 0.05$]. Collapsed across stimulus type and site, mean amplitudes were greater in TLE patients than controls; collapsed across group and site, deviant amplitudes were greater than standard amplitudes. No significant interaction between factors was observed. In addition, separate two-way repeated-measures ANOVAs were performed for deviant and standard mean amplitudes. No significant main effects of GROUP or SITE or an interaction between factors were found for deviant stimuli. Conversely, for standard stimuli a main effect of GROUP was found [$F(1, 38) = 13.65$, $p < 0.001$], with TLE patients showing greater mean amplitudes than controls (see Fig. 1 and Table 2). No main effect of SITE or an interaction between GROUP and SITE was found for standard stimuli.

A two-way repeated measures ANOVA for MMP peak latency based on the difference waveform revealed a significant main effect of GROUP ($F(1, 38) = 4.39$, $p < 0.05$) and SITE ($F(1, 38) = 7.65$, $p < 0.01$), indicating that MMP peak latency was delayed in TLE patients relative to controls, and that both groups displayed delayed MMP peak latencies in the right relative to left mastoid (see Fig. 2 and Table 2). There was a trend toward a significant interaction between GROUP and SITE [$F(1, 38) = 3.88$, $p = 0.056$], although the difference did not reach a significant level.

MMN/P and epileptic seizures

At frontocentral sites, a 2 (STIMULUS: standard vs. deviant) × 2 (SITE: Fz vs. Cz) × 2 (SUBGROUP: intractable vs. remission) repeated-measures ANOVA for mean amplitudes of standard and deviant waveforms in the range of 100–250 ms revealed a significant main effect of STIMULUS [$F(1, 38) = 9.44$, $p < 0.01$], such that deviant amplitudes were greater than standard amplitudes (see Table 3). No main effect of GROUP or interaction between STIMULUS and SUBGROUP was observed. For MMN peak latency, a 2 (SITE: Fz vs. Cz) × 2 (SUBGROUP: intractable vs. remission) repeated measures ANOVA revealed no significant main effects or interactions.

At mastoid sites, a three-way repeated measures ANOVA for mean amplitudes of standard and deviant stimuli revealed no significant main effects or interactions between factors. With respect to MMP peak latency, a two-way repeated measures ANOVA revealed a significant main effect of SITE [$F(1, 18) = 7.06$, $p < 0.05$], reflecting longer latencies in both groups for right than left mastoid (see Table 3). No main effect of SUBGROUP or interaction between SITE and SUBGROUP was observed.

Discussion

In response to a passive auditory oddball task, patients with TLE exhibited patterns of cortical activity that differed from control subjects in several ways. First, at frontocentral sites, MMN was enhanced in TLE patients relative to controls, as revealed by a significant GROUP by STIMULUS interaction for mean amplitude. Secondly, at mastoid sites, TLE patients showed greater standard waveform amplitudes than controls. Finally, in addition to amplitude differences between groups, analyses revealed longer MMN/P peak latencies in TLE patients relative to controls at both frontocentral and mastoid sites.

A number of researchers have noted that mismatch potentials recorded from mastoid electrodes may exhibit characteristics different from those of MMN recorded from frontal electrodes (Baldeweg et al., 2002; Sato et al., 2002). Early studies of MMN identified a single dipole generator within the bilateral superior temporal gyri (STG) in the vicinity of Heschl's gyri (Scherg et al., 1989). Toward the mastoids, an inversion of polarity is typically observed and has been considered evidence for the generation of MMN in the temporal lobe (Sams et al., 1985). However, more recently it has been suggested that the single dipole model may not account for all the data, and that more than one source may contribute to the scalp MMN (Giard et al., 1994). To this end, multichannel MEG and EEG studies (Rinne et al., 2000) as well as intracranial recordings (Rosburg et al., 2005) have identified additional generators in the frontal cortex. In the latter study, MMN was observed in two patients at electrode contacts over lateral inferior frontal cortex and in one patient in a frontal interhemispheric electrode strip, providing evidence for the participation of frontal gyri in MMN generation. Recent observations have led to the view that temporal electrodes mainly detect mismatch sources in the superior temporal lobe, including perhaps its lateral surface, while electrodes over the frontal scalp may detect signals from putative frontal generators (Escera et al., 2003; Näätänen et al., 2007).

In addition to debate surrounding the number of MMN generators, the specific neural mechanisms underlying MMN generation also remain controversial. Two major competing hypotheses, the model adjustment hypothesis and the adaptation hypothesis, are considered below in relation to the current findings.

To date, the most commonly suggested mechanism underlying MMN generation is a pre-attentive sensory memory mechanism (Tiitinen et al., 1994) posited to automatically compare present auditory input and memory traces of previous sounds (Näätänen et al., 2007). More specifically, it has been suggested that MMN may reflect on-line modifications of a perceptual model that is updated when auditory input does not match its predictions (Näätänen and Winkler, 1999), a hypothesis known as the model-adjustment hypothesis. Based on this model, MMN is thought to result from two underlying functional processes: a sensory memory mechanism arising from temporal generators and an automatic attention-switching process arising from frontal generators (Giard et al., 1990). Providing support for this model, Escera et al. (2003) demonstrated evidence for prefrontal cortex involvement in providing top-down modulation of a deviance detection system in the temporal cortex. With respect to

Please cite this article in press as: Miyajima, M., et al., Abnormal mismatch negativity for pure-tone sounds in temporal lobe epilepsy. Epilepsy Res. (2011), doi:10.1016/j.eplepsyres.2011.01.009

the current study, findings of enhanced MMN at frontocentral sites in TLE patients might thus be interpreted as frontal lobe hyperexcitability to compensate for temporal lobe dysfunction. That is, a larger number of synchronously activated frontal neurons may be required for successful automatic attention-switching in TLE patients than in controls, due to impairment of a initial sensory memory mechanism in the temporal lobe.

An alternative mechanism recently proposed by Jääskeläinen et al. (2004) suggests that MMN results from a much simpler mechanism of local neuronal adaptation in the auditory cortex. According to the adaptation hypothesis, reduced responsiveness in the auditory cortex during continuous stimulation is sufficient to explain the generation of an apparent MMN. In the current study, although deviant – standard differences (i.e., MMP) at mastoid sites did not significantly differ between the two groups, greater standard waveform amplitudes were observed in patients than in controls. With respect to the adaptation hypothesis, such findings may reflect poor neuronal adaptation in the temporal lobe such that repeated presentation of standard stimuli does not lead to reduced responses. In other words, processing resources may continue to be allocated in TLE patients despite the repetitive nature of the standard stimuli (Myatchin et al., 2009). TLE may be characterized by excitability of the temporal lobe despite stimulus repetition, which might be related to epileptogenesis of the temporal cortex. The current results suggest that adaptation mechanism of the temporal cortex for stimuli that are subsequently repeated may be impaired in TLE.

It also bears noting that longer latency components such as P3a may have affected the pre-stimulus baseline period, in turn affecting MMN/P amplitudes given that epochs were baseline-corrected. Specifically, because we chose a short SOA (500 ms), standard trials preceded by a deviant trial may have had different pre-stimulus baseline periods than those preceded by another standard trial. Although P300 abnormalities in TLE are controversial, studies in chronic TLE patients typically report trends toward lower P300 amplitudes relative to controls (e.g., Drake et al., 1986; Tuunainen et al., 1995; Abubakr and Wambacq, 2003). To avoid potential confounds related to P3a, future studies should exclude standard trials preceded by deviant trials from averaging.

In addition to amplitude differences between TLE patients and controls, a second key difference was an increase in MMN/P latency in TLE patients, consistent with previous reports (Lin et al., 2007; though see Duncan et al., 2009, for reports of normal auditory P300 latencies in patients with complex partial seizures). Because ERPs provide a chronological measure of brain function and ERP latencies are thought to indicate timing of covert neuronal events in which certain subroutines in the brain are activated (Kok, 1997), increased MMN/P latencies in TLE patients in the current study may be the result of an early but not later slowing in auditory information processing speed.

Furthermore, in TLE patients the MMN component persisted longer at frontocentral sites than in controls, consistent with previous findings by Gene-Cos et al. (2005). The authors argue that prolonged MMN duration might point to difficulty mainly in "the closure mechanism of the MMN process". They suggest that this information processing dysfunction could be related to concentration and memory difficulties observed in TLE patients, given that patients may spend more time evaluating stimulus novelty than controls and may experience difficulty switching attention from one stimulus to another difficult (Piazzini et al., 2006). Such findings in epilepsy patients are in agreement with previous studies in which barely discriminable tones elicited delayed MMN peaks (Näätänen and Alho, 1995; Inouchi et al., 2004) with delays increasing as the magnitude of deviation decreased (Yabe et al., 2001; Inouchi et al., 2004).

Interestingly, collapsed across subject groups, MMP was delayed in the right mastoid compared with the left. Because of the small number of patients whose epileptic focus was clearly lateralized, statistical analyses could not be conducted to evaluate the relationship between MMP latency and laterality of epileptic focus. Furthermore, given that laterality effects have not been reported previously with respect to MMP latency in healthy adults, further investigation is warranted before drawing strong conclusions about this finding.

Finally, our patient subgroup analysis investigating the relationship between seizures and MMN/P did not reveal any significant differences between groups, suggesting that the occurrence or absence of seizures in the months leading up to the experiment did not significantly affect MMN/P.

Because all patients were being treated with AEDs at the time of data collection, it bears noting that use of AEDs may have affected MMN/P amplitudes and latencies. It has been shown, for example, that anti-epileptic medication can have an effect on motor reaction times and on latencies in ERP studies (Lagae, 2006; Myatchin et al., 2009), as well as an overall dampening effect on amplitudes (Rosburg et al., 2005). Benzodiazepines, which are also used as AEDs, have been found to reduce MMN amplitude (Rosburg et al., 2004). To this end, the current finding of enhanced MMN amplitudes in TLE patients cannot be explained as a simple dampening effect of AEDs, though further studies will be required to better address the effects of AEDs on MMN. Finally, although all patients reported normal hearing levels, it is possible that MMN/P was affected by subclinical differences in auditory discriminative abilities between patients and controls.

Taken together, results from the present study reveal clear cortical abnormalities in TLE patients that have not been well-characterized previously by conventional EEG. In TLE patients, enhanced MMN at frontocentral sites and greater positivity at mastoid sites of standard waveforms may be interpreted in terms of increased activation of the same neuronal population as in controls, or activation of extra neuronal circuits. In conclusion, the current study extends previous findings of impaired short and long-term memory in TLE patients (Butler and Zeman, 2008; McCagh et al., 2009) by revealing that initial sensory memory is impaired in TLE as well. Our findings indicate that MMN/P can be useful as a physiological probe of pre-attentitve sensory memory for tones in TLE.

Acknowledgements

We appreciate the advice and expertise of Dr. Hiroshi Otsubo and Dr. Tomoyuki Akiyama. We are also grateful to Dr. Kikuo

Please cite this article in press as: Miyajima, M., et al., Abnormal mismatch negativity for pure-tone sounds in temporal lobe epilepsy. Epilepsy Res. (2011), doi:10.1016/j.eplepsyres.2011.01.009

Ohno, Dr. Motoki Inaji, Atsushi Shirasawa, Michi Baba, Yasuka Emori, Ayasa Matsuda, Mina Yamada, and the staff at Hara Clinic for their help and assistance.

References

Abubakr, A., Wambacq, I., 2003. The localizing value of auditory event-related potentials (P300) in patients with medically intractable temporal lobe epilepsy. Epilepsy Behav. 4, 692–701.

Baldeweg, T., Klugman, A., Gruzelier, J.H., Hirsch, S.R., 2002. Impairment in frontal but not temporal components of mismatch negativity in schizophrenia. Int. J. Psychophysiol. 43, 111–122.

Baldeweg, T., Williams, J.D., Gruzelier, J.H., 1999. Differential changes in frontal and sub-temporal components of mismatch negativity. Int. J. Psychophysiol. 33, 143–148.

Boatman, D.F., Trescher, W.H., Smith, C., Ewen, J., Los, J., Wied, H.M., Gordon, B., Kossoff, E.H., Gao, Q., Vining, E.P., 2008. Cortical auditory dysfunction in benign rolandic epilepsy. Epilepsia 49, 1018–1026.

Borghetti, D., Pizzanelli, C., Maritato, P., Fabbrini, M., Jensen, S., Iudice, A., Murri, L., Sartucci, F., 2007. Mismatch negativity analysis in drug-resistant epileptic patients implanted with vagus nerve stimulator. Brain Res. Bull. 73, 81–85.

Butler, C.R., Zeman, A.Z., 2008. Recent insights into the impairment of memory in epilepsy: transient epileptic amnesia, accelerated long-term forgetting and remote memory impairment. Brain 131 (Pt. 9), 2243–2263.

Commission on Classification and Terminology of the International League Against Epilepsy, 1989. Proposal for revised classification of epilepsies and epileptic syndromes. Commission on Classification and Terminology of the International League Against Epilepsy. Epilepsia 30, 389–399.

Cowan, N., Winkler, I., Wolgang, T., Näätänen, R., 1993. Memory prerequisites of mismatch negativity in the auditory event-related potential (ERP). J. Exp. Psychol. Learn. Mem. Cogn. 19, 909–921.

Dietl, T., Kurthen, M., Kirch, D., Staedtgen, M., Schaller, C., Elger, C.E., Grunwald, T., 2008. Limbic event-related potentials to words and pictures in the presurgical evaluation of temporal lobe epilepsy. Epilepsy Res. 78, 207–215.

Drake Jr., M.E., Burgess, R.J., Gelety, T.J., Ford, C.E., Brown, M.E., 1986. Long-latency auditory event-related potentials in epilepsy. Clin. Electroencephalogr. 17, 10–13.

Duman, O., Kizilay, F., Fettahoglu, C., Ozkaynak, S., Haspolat, S., 2008. Electrophysiologic and neuropsychologic evaluation of patients with centrotemporal spikes. Int. J. Neurosci. 118, 995–1008.

Duncan, C.C., Mirsky, A.F., Lovelace, C.T., Theodore, W.H., 2009. Assessment of the attention impairment in absence epilepsy: comparison of visual and auditory P300. Int. J. Psychophysiol. 73, 118–122.

Escera, C., Yago, E., Corral, M.J., Corbera, S., Nuñez, M.I., 2003. Attention capture by auditory significant stimuli: semantic analysis follows attention switching. Eur. J. Neurosci. 18, 2408–2412.

Gene-Cos, N., Pottinger, R., Barrett, G., Trimble, M.R., Ring, H.A., 2005. A comparative study of mismatch negativity (MMN) in epilepsy and non-epileptic seizures. Epileptic Disord. 7, 363–372.

Giard, M.H., Perrin, F., Pernier, J., Bouchet, P., 1990. Brain generators implicated in the processing of auditory stimulus deviance: a topographic event-related potential study. Psychophysiology 27, 627–640.

Giard, M.H., Perrin, F., Echallier, J.F., Thévenet, M., Froment, J.C., Pernier, J., 1994. Dissociation of temporal and frontal components in the human auditory N1 wave: a scalp current density and dipole model analysis. Electroencephalogr. Clin. Neurophysiol. 92, 238–252.

Honbolygó, F., Csépe, V., Fekésházy, A., Emri, M., Márián, T., Sárközy, G., Kálmánchey, R., 2006. Converging evidences on language impairment in Landau–Kleffner syndrome revealed by behavioral and brain activity measures: a case study. Clin. Neurophysiol. 117, 295–305.

Inouchi, M., Kubota, M., Ohta, K., Shirahama, Y., Takashima, A., Horiguchi, T., Matsushima, E., 2004. Human auditory evoked mismatch field amplitudes vary as a function of vowel duration in healthy first-language speakers. Neurosci. Lett. 366, 342–346.

Jääskeläinen, I.P., Ahveninen, J., Bonmassar, G., Dale, A.M., Ilmoniemi, R.J., Levänen, S., Lin, F.H., May, P., Melcher, J., Stufflebeam, S., Tiitinen, H., Belliveau, J.W., 2004. Human posterior auditory cortex gates novel sounds to consciousness. Proc. Natl. Acad. Sci. U.S.A. 101, 6809–6814.

Kasai, K., Nakagome, K., Itoh, K., Koshida, I., Hata, A., Iwanami, A., Fukuda, M., Kato, N., 2002. Impaired cortical network for preattentive detection of change in speech sounds in schizophrenia: a high-resolution event-related potential study. Am. J. Psychiatry 159, 546–553.

Kok, A., 1997. Event-related-potential (ERP) reflections of mental resources: a review and synthesis. Biol. Psychol. 45, 19–56.

Lagae, L., 2006. Cognitive side effects of anti-epileptic drugs. The relevance in childhood epilepsy. Seizure 5, 235–241.

Lin, Y.Y., Hsiao, F.J., Shih, Y.H., Yiu, C.H., Yen, D.J., Kwan, S.Y., Wong, T.T., Wu, Z.A., Ho, L.T., 2007. Plastic phase-locking and magnetic mismatch response to auditory deviants in temporal lobe epilepsy. Cereb. Cortex 17, 2516–2525.

McCagh, J., Fisk, J.E., Baker, G.A., 2009. Epilepsy, psychosocial and cognitive functioning. Epilepsy Res. 86, 1–14.

Metz-Lutz, M.N., Filippini, M., 2006. Neuropsychological findings in Rolandic epilepsy and Landau–Kleffner syndrome. Epilepsia 47 (Suppl. 2), P71–75.

Milovanov, R., Huotilainen, M., Esquef, P.A.A., Alku, P., Välimäki, V., Tervaniemi, M., 2009. The role of musical aptitude and language skills in preattentive duration processing in school-aged children. Neurosci. Lett. 460, 161–165.

Miyajima, M., Hara, K., Iino, H., Ohta, K., Maehara, T., Hara, M., Matsuura, M., Matsushima, E., 2009. Auditory mismatch negativity in frontal lobe epilepsy with auditory triggered seizure: a case study. In: The 39th Meeting of Japanese Society of Clinical and Neurophysiology , Kokura, Japan (in Japanese).

Myatchin, I., Mennes, M., Wouters, H., Stiers, P., Lagae, L., 2009. Working memory in children with epilepsy: an event-related potentials study. Epilepsy Res. 86, 183–190.

Näätänen, R., Gaillard, A.W., Mäntysalo, S., 1978. Early selective-attention effect on evoked potential reinterpreted. Acta Psychol. (Amst.) 42, 313–329.

Näätänen, R., Paavilainen, P., Alho, K., Reinikainen, K., Sams, M., 1989. Do event-related potentials reveal the mechanism of the auditory sensory memory in the human brain? Neurosci. Lett. 98, 217–221.

Näätänen, R., Alho, K., 1995. Mismatch negativity—a unique measure of sensory processing in audition. Int. J. Neurosci. 80, 317–337.

Näätänen, R., Winkler, I., 1999. The concept of auditory stimulus representation in cognitive neuroscience. Psychol. Bull. 125, 826–859.

Näätänen, R., 2000. Mismatch negativity (MMN): perspectives for application. Int. J. Psychophysiol. 37, 3–10.

Näätänen, R., Paavilainen, P., Rinne, T., Alho, K., 2007. The mismatch negativity (MMN) in basic research of central auditory processing: a review. Clin. Neurophysiol. 118, 2544–2590.

Pekkonen, E., Hirvonen, J., Jääskeläinen, I.P., Kaakkola, S., Huttunen, J., 2001. Auditory sensory memory and the cholinergic system: implications for Alzheimer's disease. NeuroImage 14, 376–382.

Please cite this article in press as: Miyajima, M., et al., Abnormal mismatch negativity for pure-tone sounds in temporal lobe epilepsy. Epilepsy Res. (2011), doi:10.1016/j.eplepsyres.2011.01.009

Pfefferbaum, A., Roth, W.T., Ford, J.M., 1995. Event-related potentials in the study of psychiatric disorders. Arch. Gen. Psychiatry 52, 559–563.

Piazzini, A., Turner, K., Chifari, R., Morabito, A., Canger, R., Canevini, M.P., 2006. Attention and psychomotor speed decline in patients with temporal lobe epilepsy: a longitudinal study. Epilepsy Res. 72, 89–96.

Rinne, T., Alho, K., Ilmoniemi, R.J., Virtanen, J., Näätänen, R., 2000. Separate time behaviors of the temporal and frontal mismatch negativity sources. NeuroImage 12, 14–19.

Rosburg, T., Marinou, V., Haueisen, J., Smesny, S., Sauer, H., 2004. Effects of lorazepam on the neuromagnetic mismatch negativity (MMNm) and auditory evoked field component N100m. Neuropsychopharmacology 29, 1723–1733.

Rosburg, T., Trautner, P., Dietl, T., Korzyukov, O.A., Boutros, N.N., Schaller, C., Elger, C.E., Kurthen, M., 2005. Subdural recordings of the mismatch negativity (MMN) in patients with focal epilepsy. Brain 128, 819–828.

Salisbury, D.F., Kuroki, N., Kasai, K., Shenton, M.E., McCarley, R.W., 2007. Progressive and interrelated functional and structural evidence of post-onset brain reduction in schizophrenia. Arch. Gen. Psychiatry 64, 521–529.

Sams, M., Hämäläinen, M., Antervo, A., Kaukoranta, E., Reinikainen, K., Hari, R., 1985. Cerebral neuromagnetic responses evoked by short auditory stimuli. Electroencephalogr. Clin. Neurophysiol. 61, 254–266.

Sato, Y., Yabe, H., Todd, J., Michie, P., Shinozaki, N., Sutoh, T., Hiruma, T., Nashida, T., Matsuoka, T., Kaneko, S., 2002. Impairment in activation of a frontal attention-switch mechanism in schizophrenic patients. Biol. Psychol. 62, 49–63.

Scherg, M., Vajsar, J., Picton, T.W., 1989. A source analysis of the late human auditory evoked potentials. J. Cogn. Neurosci. 1, 336–355.

Stefanics, G., Haden, G.P., Sziller, I., Balázs, L., Beke, A., Winkler, I., 2009. Newborn infants process pitch intervals. Clin. Neurophysiol. 120, 304–308.

Tiitinen, H., May, P., Reinikainen, K., Näätänen, R., 1994. Attentive novelty detection in humans is governed by pre-attentive sensory memory. Nature 372, 90–92.

Tuunainen, A., Nousiainen, U., Pilke, A., Mervaala, E., Riekkinen, P., 1995. Lateralization of event-related potentials during discontinuation of antiepileptic medication. Epilepsia 36, 262–269.

Usui, K., Ikeda, A., Nagamine, T., Matsubayashi, J., Matsumoto, R., Hiraumi, H., Kawamata, J., Matsuhashi, M., Takahashi, R., Fukuyama, H., 2009. Abnormal auditory cortex with giant N100m signal in patients with autosomal dominant lateral temporal lobe epilepsy. Clin. Neurophysiol. 120, 1923–1926.

Yabe, H., Koyama, S., Kakigi, R., Gunji, A., Tervaniemi, M., Sato, Y., Kaneko, S., 2001. Automatic discriminative sensitivity inside temporal window of sensory memory as a function of time. Cogn. Brain Res. 12, 39–48.

Please cite this article in press as: Miyajima, M., et al., Abnormal mismatch negativity for pure-tone sounds in temporal lobe epilepsy. Epilepsy Res. (2011), doi:10.1016/j.eplepsyres.2011.01.009

幻覚妄想の分子イメージング
—統合失調症とパーキンソン病の精神病症状—

大久保善朗
Yoshiro Okubo
日本医科大学精神医学教室 主任教授

はじめに

脳内のドパミンが減少するパーキンソン病（PD）では，薬剤によるドパミン補充療法を行う際に，副作用として幻覚妄想などの精神病症状を呈することがある。精神病症状は，「実際には存在しない対象を知覚する」幻覚と「誤った判断や意味づけを確信する」妄想を意味する。精神病症状を呈する代表的な精神疾患である統合失調症ではPDとは逆に脳内でドパミンの増加が想定されている。本稿では，分子イメージングを用いた統合失調症の研究成果を紹介しながら，統合失調症では主症状として生じ，PDでは薬剤性の副作用として生じる幻覚妄想の病態について考える。

幻覚妄想の分子イメージング —統合失調症のドパミン仮説の検証—

ドパミン仮説は，統合失調症の脳内にドパミンの過剰伝達を想定する病態仮説であり，抗精神病薬の臨床的力価とドパミンD2遮断作用の間には直線的な相関関係が存在すること，統合失調症の死後脳でD2受容体が2～3倍に増加することが報告されたことから，特にD2受容体の異常が想定されてきた。

PET（positron emission tomography）による分子イメージングでは，[^{11}C]NMSPを用いて線条体D2受容体の増加を報告する研究が先行した。しかしながら，その後，[^{11}C]raclopride を用いた研究では健常人との差を否定する報告もあり結果は一致しなかった。多数のPET研究のメタ解析でも，せいぜい10～20%の軽度上昇が認められるという結論である。このようなPET研究の結果から，死後脳で観察された線条体D2受容体の増加は，長期の抗精神病薬の投与によるD2受容体の二次的な増加を反映している可能性も考えられている。

PETと[^{18}F]fluoro-L-Dopa を用いL-ドパの脳内への取り組みを測定することにより，ドパミン合成能を測定することができる。統合失調症群と健常対照群の線条体におけるドパミン合成能を比較した複数の報告では，統合失調症患者におけるドパミン合成能の亢進が報告されている。我々も，L-[β-^{11}C]DOPAを用いて統合失調症患者群と健康対照群を対象にPET検査（**図1左**）を行い，統合失調症患者の左尾上核においてドパミン合成能が亢進していること，視床と右側頭葉のドパミン合成能が症状の重症度と正の相関を示すことを明らかにした。さらに，[^{11}C]PE2IはドパミントランスポーターをPET測定するために近年開発されたPETリガンド（**図1右**）であるが，統合失調症では視床のドパミントランスポーターが増加しており，その増加は精神症状の重症度と正の相関を示していた[1]。

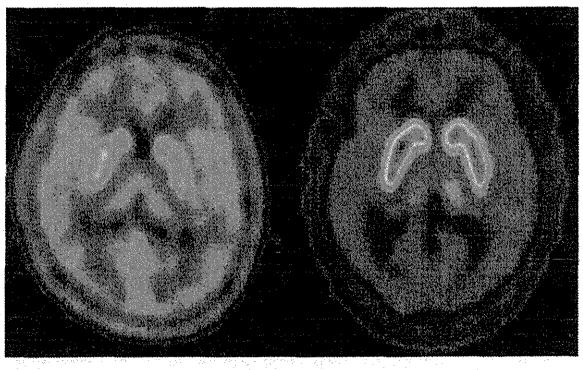

図1　PETによるシナプス前ドパミン機能の測定
左：L-[β-^{11}C]DOPAによるドパミン合成能の評価。
右：[^{11}C]PE2Iによるドパミントランスポーターの評価。
左右とも健康人の画像。

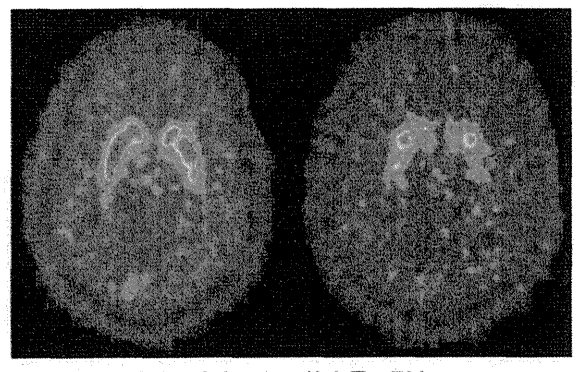

図2　PETを用いたドパミン放出量の測定
[^{11}C]raclopride を用いたドパミン放出量の測定。
左：ベースライン。右：薬剤などの作用でドパミン放出量が増加すると[^{11}C]raclopride とドパミンの競合が起きて線条体での取り込みが低下する。

さて，幻覚妄想を引き起こす覚醒剤アンフェタミンを投与するとドパミンが放出され，シナプス間隙の内在性のドパミン濃度が高くなる。この時にPET検査でドパミンD2受容体を測定すると，放出されたドパミンによってD2受容体の結合能が低下することがわかる。このような原理を用いて，シナプスに放出されるドパミン濃度を測定することができる（**図2**）。同法を用いドパミン放出能を比較した研究では，統合失調症患者におけるドパミン放出能の亢進が報告されている[2]。

以上，統合失調症におけるドパミン合成能の亢進，ドパミントランスポーターの増加，ドパミン放出能の増加という所見は，シナプス前ドパミン機能の亢進という点で一致しており，統合失調症において，ドパミン系の機能が亢進して過剰な伝達が生じていると想定するドパミン仮説を支持している。

PDの分子イメージング

PDでは，D2受容体については統合失調症と同様に変化に乏しいことが報告されている。一方，[^{18}F]fluoro-L-Dopaで測定したL-ドパの取り込みは被殻で低下し，進行とともにさらに低下することが報告されている。また，ドパミントランスポーターについても減少することが報告されており，脳内のドパミンの減少に伴いドパミントランスポーターにダウンレギュレーションが起きると考えられている。

以上，PDのPET所見[3]については，ドパミンD2受容体に変化を認めない点は統合失調症と共通している。一方，ドパミン合成能および各種リガンドで測定されたドパミントランスポーターなど，シナプス前ドパミン機能については統合失調症とは逆に減少することが報告されている。

ドパミンD2受容体遮断と抗精神病作用およびパーキンソン症状

PETによって*in vivo*でドパミンD2受容体の測定が可能になって間もなく，抗精神病薬による治療中の患者では，抗精神病薬によって65～85％の線条体D2受容体が占有されていることが明らかになった。さらに，D2受容体占有率と臨床効果の関連を調べたところ，抗精神病作用

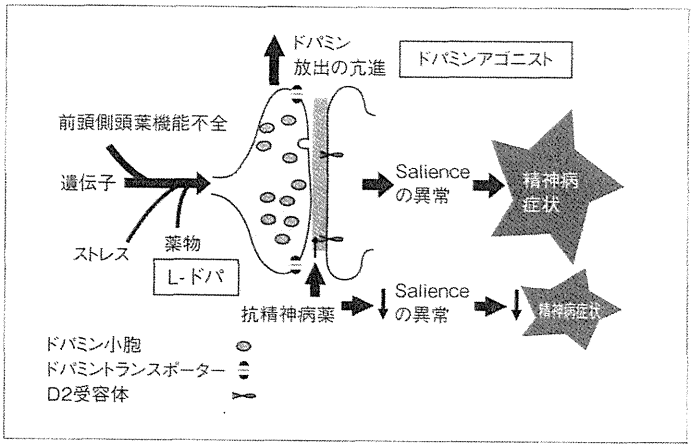

図3　ドパミン過剰と異常顕現性

の発現には70%以上のD2受容体占有が必要であるという治療閾値とともに，80%以上のD2受容体が占有されると，副作用としてパーキンソン症状が発現することが明らかになった。このような結果は，抗精神病薬が確かに統合失調症患者の脳内でD2受容体を遮断して抗精神病作用をもたらしていることを示す証拠である。また，必要以上のD2受容体を遮断すると副作用としてパーキンソン症状が出現することから，抗精神病薬の処方にあたっては副作用なく臨床効果が期待できるtherapeutic window（治療の窓）を考慮する必要性があると考えられた。

ドパミン過剰放出と幻覚妄想
—異常顕現性（aberrant salience）—

統合失調症の病態としてドパミン機能の調節が破綻して，神経伝達が過剰になっている状態が想定される。そのようなドパミンの過剰な放出がどのように幻覚や妄想に結びつくかについて，精神病症状を異常顕現性（aberrant salience）状態と捉えて説明する興味深い仮説が提案されている[1]。

顕現性（salience）とは，「突起」や「際立ち」とも訳されるもので，周囲よりも目立って認識されるものを意味する。自分にとって行動を起こす必要がある，大事なものや興味を引くものに遭遇すると，脳内ではドパミンが放出され行動を起こすような顕現性が認識されることが知られている。ドパミンを介して動機的顕現性（motivational salience）が発現するとも言われる。顕現性にはよい出来事だけでなく悪い出来事もあり，ドパミンの放出はヒトの行動の動機付けに関与している。

統合失調症においては，様々な要因により異常なドパミンの放出が起きている。したがって，現実の刺激がなく，顕現性を認めないにもかかわらず，異常な顕現性が生じる。異常な顕現性は幻聴や妄想知覚などへと結実して，異常な顕現性を説明する認知的図式として妄想が生じると想定される。したがって，抗精神病薬によってドパミン神経伝達を遮断することによって，異常な顕現性が消失し，幻覚，そして妄想が消退すると考えられる。

一方，PDではドパミン補充療法中に薬剤の副作用として精神病症状が出現する。PDでは，疾病によりドパミンの放出量自体は低下していると考えられるが，L-ドパの投与により一時的であってもドパミンの過剰な放出が起きて顕現性が亢進し幻覚妄想が発現する可能性が考えられる。また，ドパミンアゴニストによる治療は，ドパミンアゴニスト自体が異常顕現性をもたらし，幻覚や妄想に結実すると想定される（図3）。